Corn bracts loading copper sulfide for rapid adsorption of Hg(II) and sequential efficient reuse as a photocatalyst

Jiwei Wang, Lanlan Dai, Shuangying Hu, Heli Yin, Minghui Yang, Aikebaier Reheman and Guiyang Yan

ABSTRACT

Hg(II) ions in wastewater are highly toxic to the environment and human health, yet many materials to remove the ions exhibit lower adsorption efficiency, and few studies report the reuse of Hg(II)-loaded waste materials. Here, a cheap and efficient adsorbent was prepared for the removal of Hg(II) based on corn bracts (CB) loading copper sulfide (CuS), and the Hg(II)-adsorbed material was reused as a photocatalyst. By changing the adsorption variables such as pH, adsorbent dosage, Hg(II) concentration, contact time and coexisting ions, the optimum adsorption conditions were obtained. The study indicated the adsorption capacity and removal rate of CB/CuS reached 249.58 mg/g and 99.83% at pH 6 with 20 mg CB/CuS, 50 mL Hg(II) concentration (100 mg/L) and 60 min, and coexisting ions did not affect the uptake of Hg(II). The adsorption behavior of CB/CuS toward Hg(II) followed pseudo-second-order and Langmuir models, with the theoretical maximum adsorption capacity of 316.46 mg/g. Finally, we explored an alternative strategy to dispose of spent adsorbents by converting the CB/CuS/HgS into a photocatalyst for the degradation of rhodamine B, with a removal rate of 98%. Overall, this work not only develops a promising material for the treatment of Hg(II)-containing wastewater, but opens up a new approach for the use of the waste adsorbent.

Key words | adsorption, corn bracts, CuS, degradation, Hg(II) ions, rhodamine B

Jiwei Wang
Lanlan Dai
Shuangying Hu
Aikebaier Reheman
Fujian Province University Engineering Research Center of Mindong She Medicine, Medical College,
Ningde Normal University,
Ningde, Fujian 352100,
China

Heli Yin
Minghui Yang
Guiyang Yan (corresponding author)
Fujian Province University Key Laboratory of Green Energy and Environment Catalysis,
Ningde Normal University,
Ningde, Fujian 352100,
China
E-mail: *ygyfjnu@163.com*

HIGHLIGHTS

- Corn bracts as a carrier of CuS was designed for rapid uptake of Hg(II).
- The removal rate of the adsorbent could reach 99.83% in only 60 min.
- The theoretical maximum could reach 316.46 mg/g.
- Coexisting ions had no significant effect on selective Hg(II) ion removal.
- The spent adsorbent was used for photodegradation reaction.

INTRODUCTION

Due to its special physical and chemical properties, mercury has irreplaceable uses in the chemical industry, electrical industry, metallurgical enterprises and medical industry, all of which cause pollution (Zhang *et al.* 2019). Mercury in water can migrate into the atmosphere by gasification and dimethylation, and the gaseous particulate mercury in the atmosphere drifts with the wind and can fall into water bodies by sedimentation. The mercury in the soil will also be washed into surface water, which seriously

doi: 10.2166/wst.2021.181

threatens human health (Velempini & Pillay 2019). Because mercury, a heavy metal, has the characteristics of persistence, easy migration, bioaccumulation and biotoxicity, it also poses a huge threat to the ecological environment (Chen *et al.* 2019; Naushad *et al.* 2019). How to deal effectively with the mercury pollution is an important research topic in the fields of environment and materials.

Corn bracts are a low-value, and underused biomaterial, composed of lignin and cellulose, that contains abundant hydroxyl functional groups (Luo *et al.* 2017; Lin *et al.* 2019). However, as a kind of agricultural waste, corn bracts are usually destroyed by incineration, which is a serious waste of resources that also causes environmental pollution (Yang & Zhou 2012). Therefore, exploring the applications of corn bracts is a useful approach for scientific researchers.

Compared with precipitation, membrane separation, flocculation, evaporation and ion exchange, separation by adsorption has gradually attracted much attention due to its simple operation and good selectivity (Oveisi *et al.* 2017; Mohammad *et al.* 2018; Qin *et al.* 2019). At present, the most widely used adsorbents include modified mesoporous silica, carbon-based materials, clay minerals, polymer and polymeric resins (Wang *et al.* 2016; Sadegh *et al.* 2018; Jimenez-Falcao *et al.* 2020). Currently, biomaterials, such as *Scrophularia striata* stems and sugarcane bagasse, are widely used for the removal of Hg(II) due being low cost, easily available, environmentally friendly and degradable (Gupta *et al.* 2014; Dehghani *et al.* 2020), however, corn bracts have not been used as adsorbents for trace Hg(II) ions.

In recent years, MoS_2, ZnS and other metal sulfides have been used as mercury adsorption materials (Pala & Brock 2012; Yi *et al.* 2019). Although these materials exhibit high adsorption capacity, they have poor specific selectivity for Hg. Metal organic frameworks (MOFs), covalent organic frameworks (COFs) and other emerging porous nanomaterials have excellent adsorption capacities, but the problems of their slow adsorption rate, poor selectivity and high cost still need to be resolved (Yang *et al.* 2010; Huang *et al.* 2015; Zhi *et al.* 2016).

In this study, a new composite material was developed by introducing copper sulfide onto the surface of corn bracts by a simple and convenient preparation method, at low cost and gives a fast and efficient adsorption performance. Adsorption parameters including pH, initial concentration, contact time and selectivity were systematically studied, along with the adsorption mechanism of Hg onto the corn bract/copper sulfide composite.

Finally, the waste adsorbent was converted into a photocatalyst for the degradation of rhodamine B, which opens up a new way to deal with toxic waste adsorbents.

EXPERIMENTAL SECTION

Materials and instruments

Corn bracts (CB) were collected from a local farmers' market; cetyltrimethylammonium bromide (CTAB), ammonium sulfide solution (AR 20%), copper sulfate pentahydrate, calcium nitrate, magnesium nitrate, zinc nitrate, lead nitrate, copper nitrate and sodium nitrate were purchased from Tianjin Daomao Chemical Reagent Company (Tianjin, China); mercury nitrate was supplied by Guizhou Tongren Tailuier Chemical Plant (Guizhou, China).

Fourier-transform infrared spectroscopy (FT-IR) spectra were recorded using a KBr pellet in the range of 4,000–500 cm^{-1} on a PerkinElmer spectrum One (B) spectrometer. Thermogravimetric analysis (TGA) of samples was carried out using a Netzsch 209C under N_2 flow at a heating rate of 20 °C min^{-1}. The X-ray powder diffraction (XRD) spectras of samples with Cu-Kα radiation ($\lambda = 1.54$ A) at 40 kV and 40 mA were obtained with a Bruker D8 Advance equipped over a range of 1–10° (2θ). The morphology of the samples was observed using a scanning electron microscope (SEM, JEOL 6500F) and a transmission electron microscope (TEM, JEM-2000EX).

Preparation of CB/CuS

The preparation process of the CB/CuS is shown in Figure 1. Firstly, the corn bracts were dried and ground to a fine powder in a pestle. The CB powder (2 g) and CTAB (0.08 g) was added to 200 mL of deionized water under vigorous stirring, followed by sonication for 60 min. Then, a $(NH_4)_2S$ solution (1.3 g) was added to the mixture and stirred for 1 hour. After that, a solution of 0.5 g $CuSO_4{\cdot}5H_2O$ in 50 mL deionized water was added dropwise, and stirred continuously and vigorously for 3 hours. The product was obtained after centrifugation followed by ethanol/water washing and drying in vacuum at 45 °C for 24 hours. In Figure 1, the positively charged CTAB adsorbed onto the CB surface enabled the stabilization of S^{2-}, which then reacted with $CuSO_4$ to precipitate the immobilized CuS nanoparticles; the composite material was washed to remove the CTAB, leaving CB/CuS.

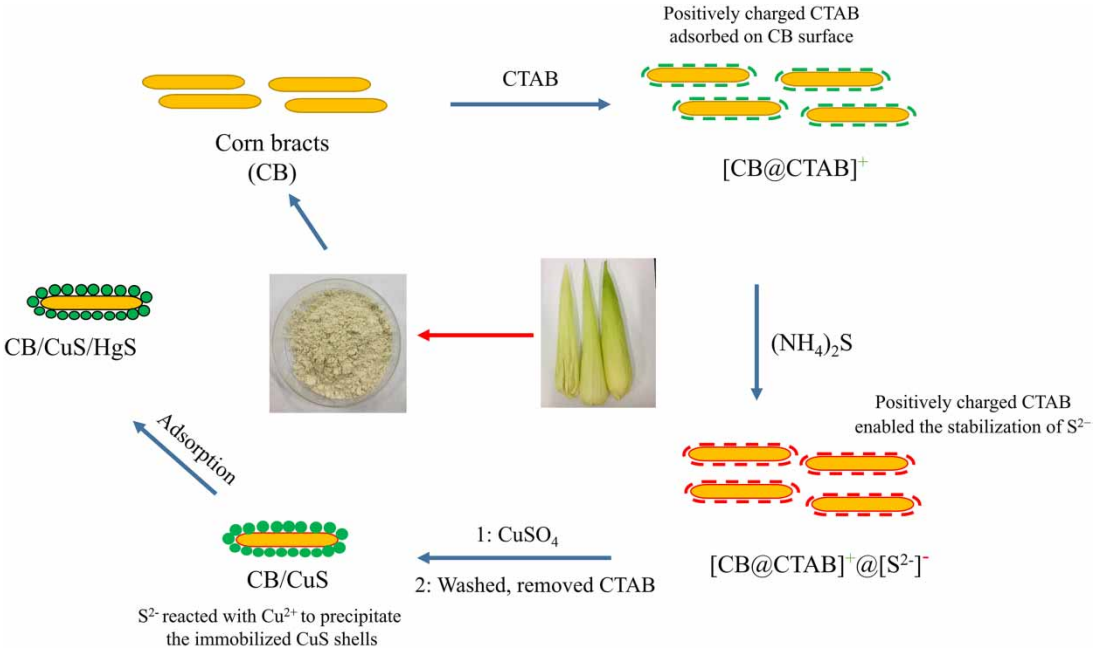

Figure 1 | The schematic depiction of the preparation of CB/CuS.

Adsorption experiment

All adsorption experiments were individually conducted in beakers at 298 K for Hg(II) uptake with 20 mg CB/CuS and 50 mL Hg(II) solution. For the effect of pH on adsorption, the 50 mL Hg(II) solutions (100 mg/L) at different pH (2–8) were adjusted with 0.8 mol/L HNO_3 and NaOH solutions. To explore the maximum adsorption capacity and adsorption isotherms, 20 mg adsorbent was added to 50 mL of various Hg(II) concentration solutions (50–300 mg/L) at pH 6 and 298 K. The effect of contact time on adsorption was explored over times ranging from 0 to 90 min with 50 mL 100 mg/L Hg(II) ion solution at pH 6.

To investigate the influence of interfering ions, 20 mg CB/CuS was added to the 50 mL Hg(II) solutions (100 mg/L) along with 0.01 M different cations at pH 6 and 298 K. After the adsorption study, the residual concentration of Hg(II) ions was monitored by UV-vis spectroscopy at the wavelength of 493 nm according to the colorimetric method of the National Standard of China (GB/T 5750.6-2006). The adsorption capacity (Q_t) and removal rate (R) of CB/CuS were calculated using Equations (1) and (2).

$$Q_t = \frac{(C_0 - C_t) \cdot V}{m} \quad (1)$$

$$R = \frac{(C_0 - C_t)}{C_0} \cdot 100\% \quad (2)$$

where C_0/C_t (mg/L), V (L), m (g), Q_t (mg/g) and R (%) are the concentration of Hg(II) ion at $t = 0$/t, volume of Hg(II) ion, adsorbent dosage, adsorption capacity and removal rate (%) at time t, respectively.

Photodegradation experiment

For the photodegradation study, 20 mg CB/CuS was added to 50 mL Hg(II) solution (200 mg/L) at 298 K and pH 6. After adsorption equilibrium, the Hg(II)-loaded adsorbent was obtained by centrifugation from aqueous solution and freeze dried for 48 hours. During the adsorption experiments, the collected spent adsorbent was added to 20 mL of rhodamine B (5 mg/L), and the mixture was stirred magnetically and placed in the dark to reach the adsorption equilibrium of rhodamine B for 60 min. After that, the system was placed in a photoreactor (halogen lamp, color temperature 6,000 K, power 150 W) and stirred at about 25 °C with 10 cm distance between the light source and the bottom of the reactor. The concentration of rhodamine B in the supernatant was determined on a double-beam UV-vis spectrophotometer at 554 nm. The corresponding degradation efficiency (K)

can be obtained using Equation (3).

$$K = \frac{A_0 - A_t}{A_0} \times 100\% \quad (3)$$

where A represents absorbance, A_0 and A_t are the absorbance of the initial solution and the solution at the time t, and K is the degradation rate.

RESULTS AND DISCUSSION

Characterization

Figure 2(a) shows the FT-IR spectra of CB and CB/CuS. The adsorption peaks at 3,432 and 2,928 cm^{-1} correspond to stretching vibrations of O-H and hydrocarbon CH_2. The peak at 1,622 cm^{-1} belongs to the stretching vibration of lignin C = O groups. The peaks at 1,037 and 1,163 cm^{-1} belong to the stretching vibration of C-O group in the alcohol (Lou *et al.* 2013; Liew *et al.* 2018). Compared with CB, after introducing copper sulfide onto the surface of the corn bracts, the FT-IR spectra of CB/CuS retained the characteristic peaks of CB, except for the weakening of peak intensity.

TGA analysis is used to describe thermal stability of materials. Figure 2(b) shows the thermal decomposition behavior of CB and CB/CuS. From the TGA curve, the mass loss belongs to the evaporation of H_2O and the solvent residue in the samples. After 200 °C, the mass loss of CB/CuS started slowly due to the thermal decomposition of CB and phase transformation of unstable CuS, indicating excellent thermal stability of CuS.

The XRD patterns of CB and CB/CuS with 2θ range of 5–90° are shown in Figure 2(c). It can be seen from Figure 2(c) that the prominent diffraction peaks at 2θ = 28.50, 31.95, 47.79 and 58.91 were exactly assigned to the (102), (103), (110) and (116) reflections of CuS, and the results indicated the CuS was introduced onto the surface of CB, which was consistent with the experiment (Sun *et al.* 2018).

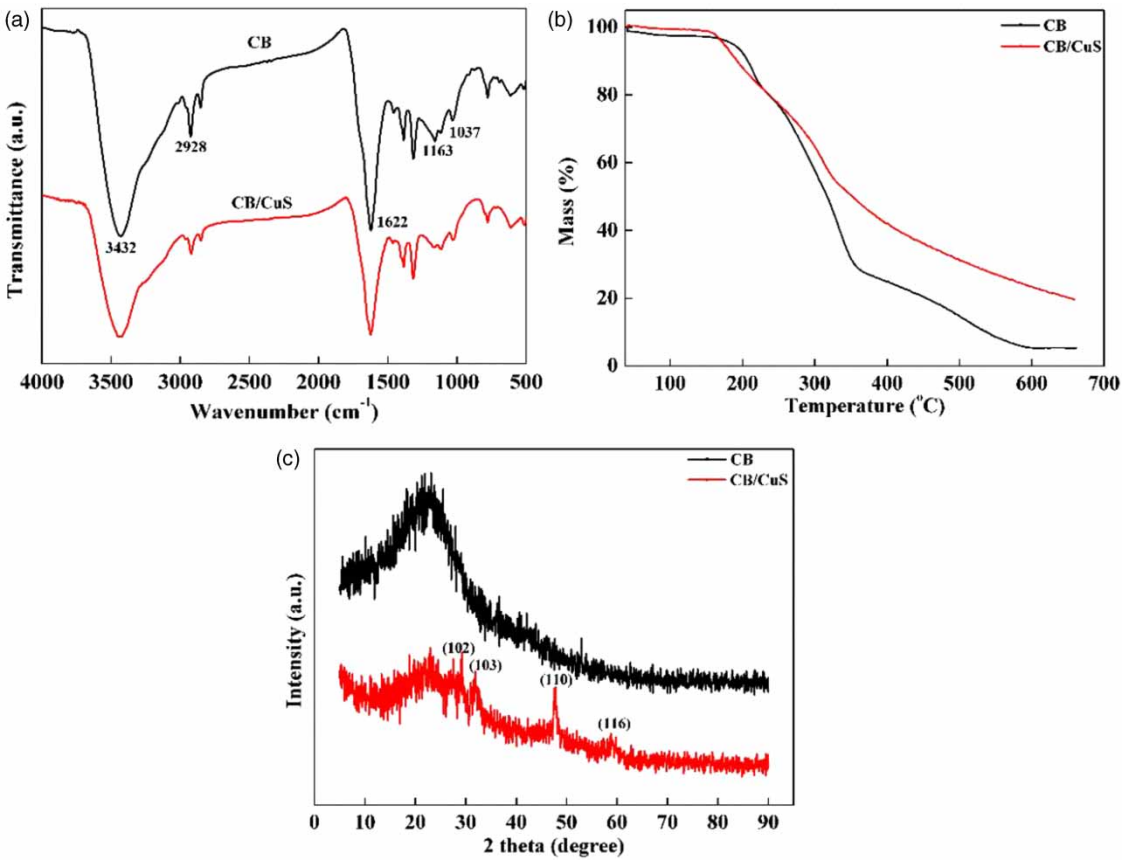

Figure 2 | FT-IR spectra of CB and CB/CuS (a); TGA curves of CB and CB/CuS (b); XRD patterns of CB and CB/CuS (c).

Figure 3 presents the surface morphology of CB and CB/CuS. The surface of CB consists of smooth and uniform blocks, as shown in Figure 3(a) and 3(b). The CuS particles attached to the CB blocks, resulting in the rough surface of CB/CuS, indicating that CuS was successfully added to the surface of CB (Figure 3(c) and 3(d)).

Adsorption study

Effect of pH

Hg(II) solution pH is a key factor affecting the adsorption behavior of materials, since it influences the ionization level of the materials and the species forms of Hg(II) ions (Fu *et al.* 2019). Figure 4(a) shows the effect of pH on the adsorption capacity of the CB/CuS. Firstly, the adsorption capacity increased sharply with pH rising from 2.0 to 3.0, then it increased slightly with pH rising from 3.0 to 6.0, finally, it decreased slightly with pH rising from 6.0 to 8.0, which could be explained as follows: At low pH values, CB loaded-CuS was readily attacked by strong acids ($pH \leq 3$), which caused the loss of particles; meanwhile, the abundant competitive H^+ ions occupied most of the binding sites of the Hg(II) ions, leading to protonated functional groups of CB. When $3 \leq pH \leq 6$, the Hg(II) solution was under weakly acidic conditions, so the S^{2-} of CuS could easily co-precipitate with Hg(II) (Sun *et al.* 2017). However, when $pH \geq 6$, the metal hydroxide species such as soluble $Hg(OH)^+$ or insoluble $Hg(OH)_2$ precipitate would be formed, which attached to the active site and hindered further adsorption (Ge & Hua 2016).

Effect of adsorbent dosage

To obtain the optimal dosage, certain amounts of adsorbent (5, 10, 15, 20 and 25 mg) were added to the 50 mL Hg(II) aqueous solution (100 mg/L) for 60 min at pH 6. The removal rate of the corresponding amount is shown in Figure 4(b), where increasing adsorbent dosage

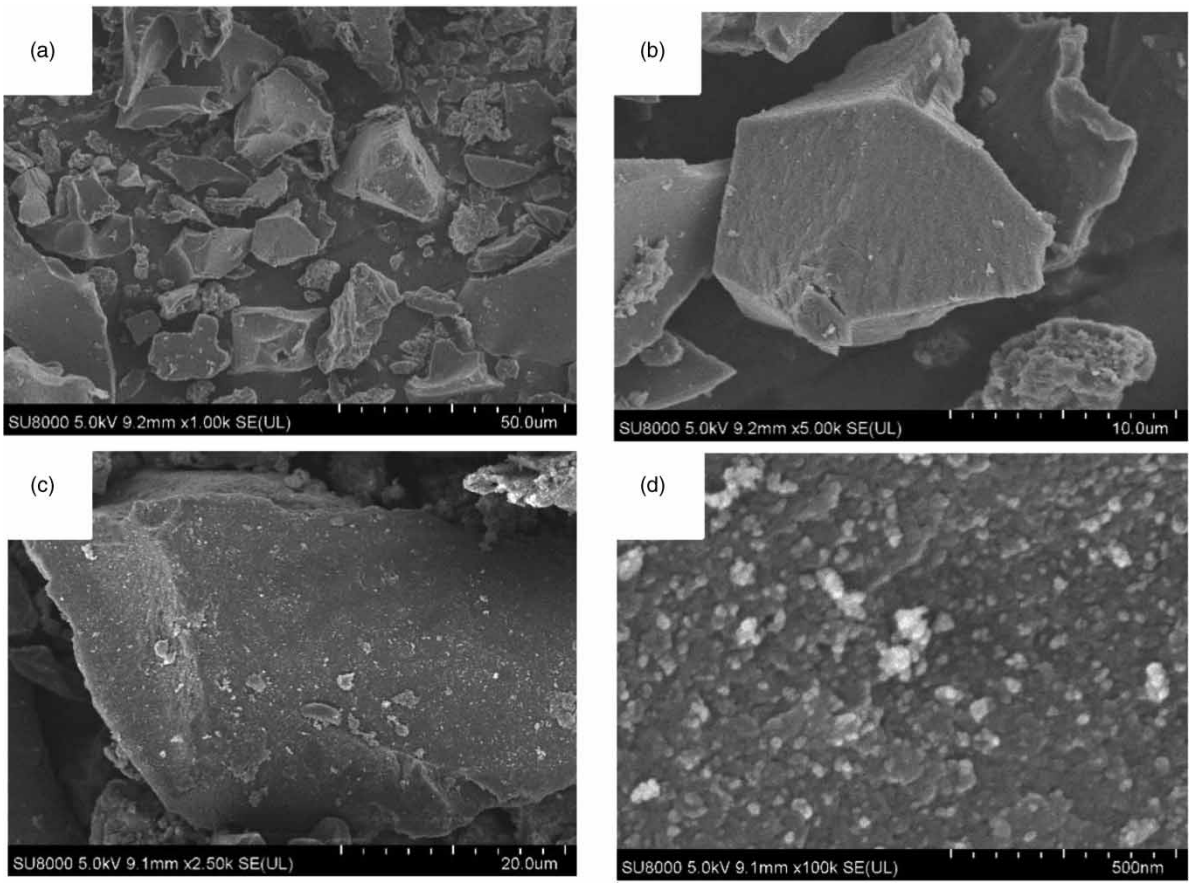

Figure 3 | SEM images of CB (a, b); CB/CuS (c, d).

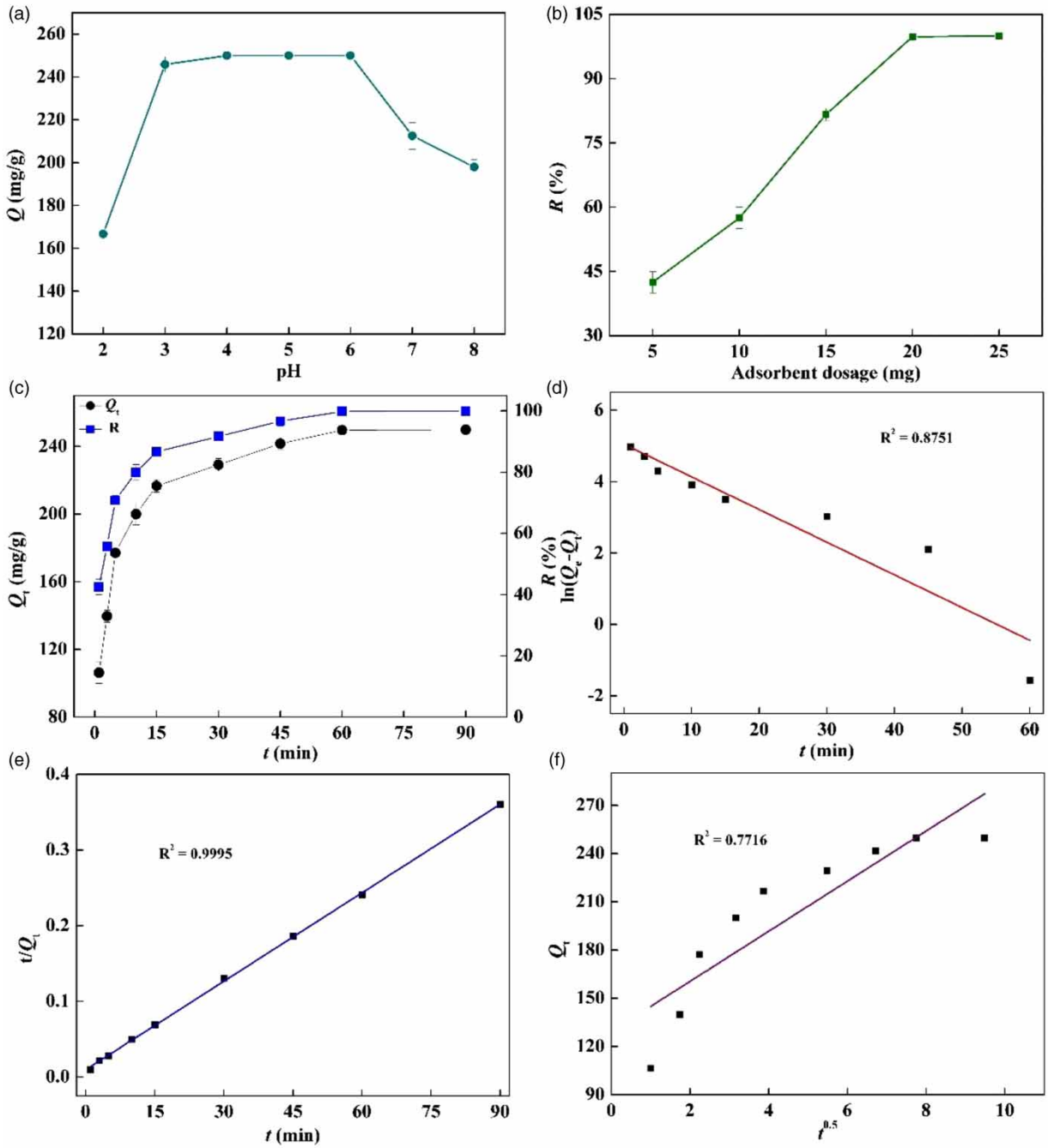

Figure 4 | (a) Effect of pH on uptake of Hg(II) ions; (b) effect of adsorbent dosage on uptake of Hg(II) ions; (c) effect of contact time on adsorption Hg(II) ions; (d) fit of kinetic data to pseudo-first-order model; (e) fit of kinetic data to pseudo-second-order model; (f) fit of kinetic data to Weber-Morris model.

resulted in the increased removal rate. Furthermore, 99% of the Hg(II) ions were adsorbed when the adsorbent dosage was 20 mg, above which the CB/CuS, indicating removal rate remained basically unchanged; therefore, 20 mg of CB/CuS was most suitable for Hg removal in aqueous solution.

Effect of contact time on adsorption and adsorption kinetics

Figure 4(c) shows the adsorption capacity (Q_t) and removal rate (R) of Hg(II) with contact time (0–90 min). Firstly, the amount of adsorbed Hg(II) rapidly increased with time,

especially between 0 and 15 min, when the adsorption capacity and removal rate reached 216.67 mg/g and 86.67%. Then their rate of increase gradually slowed to equilibrium; finally, the adsorption capacity and removal rate reached 249.58 mg/g and 99.83% after 60 min.

The pseudo-first-order, pseudo-second-order and Weber-Morris models were applied to study the mechanisms and major kinetic factors, and the corresponding parameters are shown in Table S1 (see Supplementary Information). From the fitting results of the above models shown in Figure 4(d)–4(f), it is clear that the pseudo-second-order equation was most suitable for describing the adsorption process owing to its higher correlation coefficient of ($R^2 > 0.99$) and the fact that the experimental adsorption capacity was close to the calculated value. This indicated the removal of Hg(II) ions by CB/CuS was controlled by chemisorption via substitution reaction and surface complexation.

Effect of Hg(II) concentration and adsorption isotherm

The effects of initial concentrations of Hg(II) ions on the adsorption capacity of CB/CuS are shown in Figure 5(a). In initial concentrations ranging from 50 to 300 mg/L, the maximum adsorption capacity (~316.67 mg/g) was achieved. Within the concentrations range of 50–200 mg/L, the adsorption capacity increased relatively fast due to the abundant adsorption sites across the surface of adsorbents. However, within the concentrations range of 200–300 mg/L, the rate of adsorption capacity gradually lessened, and the adsorption capacity reached equilibrium at 300 mg/L when active sites were fully occupied. The Hg(II) uptake for the series of initial concentrations fitted to the Langmuir and Freundlich models is shown in Figure 5(b) and 5(c), and the corresponding parameters are listed in Table S2 (see Supplementary Information).

It was clear that the values of the correlation coefficient of the Langmuir model ($R^2 = 0.9975$) were all much higher than

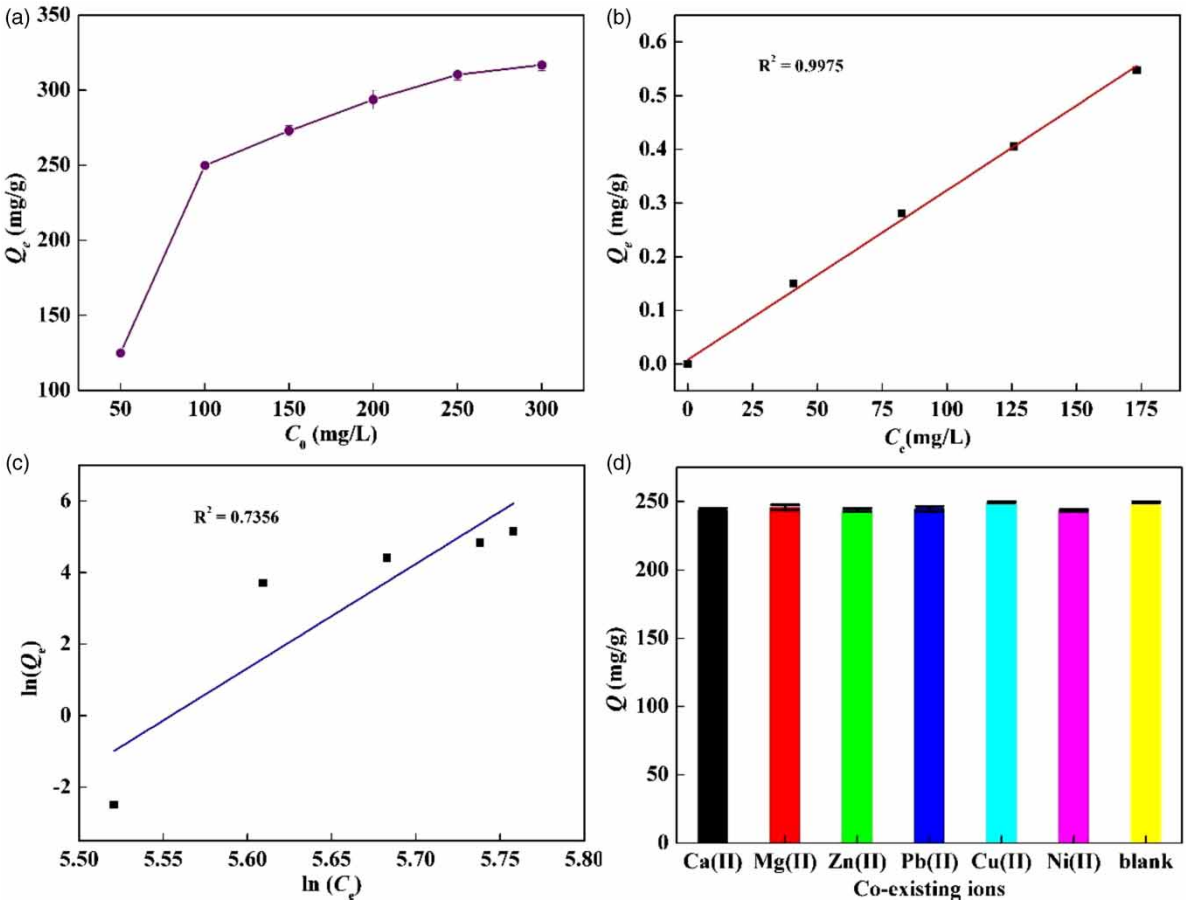

Figure 5 | (a) Effect of initial concentration on uptake of Hg(II) ions; (b) Langmuir isotherm plots; (c) Freundlich isotherm plots; (d) effect of coexisting ions on adsorption of Hg(II) ions.

that of the Freundlich model ($R^2 = 0.7356$), and the theoretical maximum adsorption capacity ($Q_{m,cal} = 316.46$ mg/g) of the Langmuir model was closer to the experimental value (Q_m of 316.67 mg/g), which indicated that the Langmuir model was more suitable to describe the adsorption behaviors of Hg(II), which was monolayer (Trikkaliotis *et al.* 2020). Compared with other adsorbents listed in Table S3 (see Supplementary Information), it is obvious that CB/CuS has a larger adsorption capacity. Thus, CB/CuS will be used as a potential candidate to remove Hg(II) from acidic aqueous solutions.

Effect of coexisted ions

There are many alkaline earth metal ions and other heavy metal ions in mercury-containing wastewater, and these cations may compete with mercury ions for active sites. Therefore, in this work, the common ions Ca(II), Mg(II), Zn(II), Pb(II), Cu(II) and Ni(II) were used to study how the presence of other cations could affect our Hg(II) removal system. It was clear that the introduction of common coexisting ions hardly inhibited the Hg(II) remove of CB/CuS (Figure 5(d)), indicating that retained its selectivity toward Hg(II) ions in the presence of the applied interference ions. The above results were explained as follows. The solubility constant of CuS is larger than that of PbS, NiS etc. but less than that of HgS, Thus, CuS is more likely to first adsorb then react with Hg(II) through the substitution reaction (Hu *et al.* 2019).

Possible adsorption mechanism of Hg(II) ions

To explore the mechanism of Hg(II) removal, XRD and FT-IR were employed to analyze the chemical compositions of CB/CuS before and after Hg(II) adsorption, and the corresponding results are shown in Figures S1 and S2 (see Supplementary Information). According to Figures S1 and S2, the XRD spectra of CB/CuS/HgS confirmed the existence of HgS on the surface of CuS, and the FT-IR of CB/CuS/HgS suggested -OH groups participated in Hg(II) adsorption. Based on this analysis, the adsorption process of CB/CuS toward Hg(II) ions is controlled by chemisorption, including through a substitution reaction and surface complexation, as shown in the following equations.

(1) Substitution reaction, resulting in the formation of HgS on the surface of CuS:

$$CuS + Hg^{2+} \rightarrow HgS + Cu^{2+}$$

(2) Surface complexation, resulting in the exchange or sharing of electrons between Hg(II) and the reactive sites:

$$\equiv CuS + Hg(II) \rightarrow \equiv CuS - Hg(II)$$

$$(CB) - OH + Hg(II)HO - (CB) \rightarrow (CB) - OH \cdots Hg(II) \cdots HO - (CB)$$

Photodegradation study

In this work, after adsorption experiments, we tried to convert CB/CuS/HgS to an active photocatalyst for the degradation of rhodamine B. Firstly, the collected spent adsorbent (10 mg) was added to 20 mL of rhodamine B (5 mg/L), stirred magnetically and placed in the dark for 60 min to achieve the adsorption equilibrium of rhodamine B; the results are shown in Figure 6. Compared with CB/CuS (47%), the removal rate of CB/CuS/Hg(II) reached 98% at 420 min, which indicated the synergistic effect of HgS on the surface of material and that CuS improved the range of spectral response and photoluminescence efficiency, which opened up a new way for the disposal of spent adsorbent in the photodegradation reaction of organic dyes.

CONCLUSIONS

In conclusion, we constructed a cheap and efficient material for the adsorption of Hg(II) and subsequently developed the spent adsorbent into an active photocatalyst for the degradation rhodamine B. The morphology and structure of

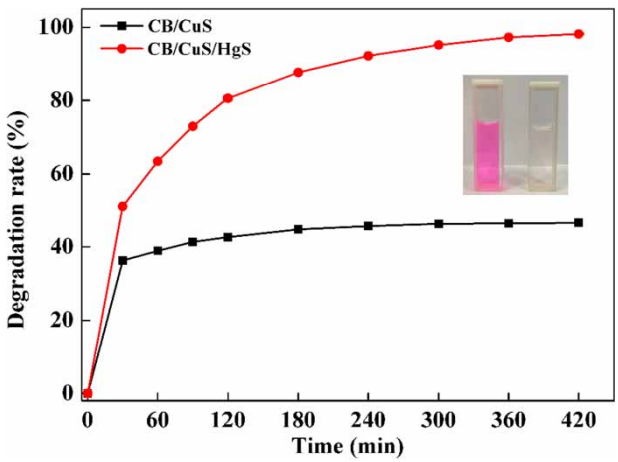

Figure 6 | Degradation rates of CB/CuS/Hg(II) and CB/CuS with time.

CB/CuS was determined successfully by FT-IR, XRD, TGA and SEM. CB/CuS showed a great efficiency for Hg(II) adsorption from aqueous solution, and its adsorption capacity and removal rate could reach 249.58 mg/g and 99.83% after 60 min at pH 6 with 50 mL of 100 mg/L Hg(II) ions. It showed excellent selectivity toward Hg(II) ions. In addition, the adsorption process followed second-order kinetics, fitted the Langmuir isotherm adsorption model with a theoretical maximum of 316.46 mg/g, and was controlled by chemisorption, including through a substitution reaction and surface complexation. Finally, the used adsorbent was used as a photocatalyst to degrade rhodamine B, with removal rate of 98%. Our work has produced a novel, fast and effective adsorbent for Hg(II) ions with excellent selectivity and reusability. We have also suggested a viable option for the reuse of the waste for photodegradation.

FUNDING STATEMENT

College Student Innovation and Entrepreneurship Training Program (202010398004), Scientific Research Fund project of Ningde Normal University (2020Z02, 2019ZX405, 2020ZX502, 2018Y06, 2018T02), and Fujian Natural Science Foundation (2019J0106).

DATA AVAILABILITY STATEMENT

All relevant data are included in the paper or its Supplementary Information.

REFERENCES

Chen, G., Li, X., Zhou, L., Xia, S. & Yu, L. 2019 Mechanism insights into Hg(II) adsorption on kaolinite(001) surface: a density functional study. *Appl. Surf. Sci.* **488**, 494–502.

Dehghani, M., Nozari, M., Golkari, I., Rostami, N. & Shiri, M. A. 2020 Adsorption of mercury(II) from aqueous solution using dried *Scrophularia striata* stems: adsorption and kinetic studies. *Desalin. Water Treat.* **203**, 1–13.

Fu, Y., Sun, Y., Chen, Z., Ying, S., Wang, J. & Hu, J. 2019 Functionalized magnetic mesoporous silica/poly(m-aminothiophenol) nanocomposite for Hg(II) rapid uptake and high catalytic activity of spent Hg(II) adsorbent. *Sci. Total Environ.* **691**, 664–674.

Ge, H. & Hua, T. 2016 Synthesis and characterization of poly(maleic acid)-grafted crosslinked chitosan nanomaterial with high uptake and selectivity for Hg(II) sorption. *Carbohyd. Polym.* **153**, 246–252.

Gupta, A., Vidyarthi, S. R. & Sankararamakrishnan, N. 2014 Thiol functionalized sugarcane bagasse – A low cost adsorbent for mercury remediation from compact fluorescent bulbs and contaminated water streams. *J. Environ. Chem. Eng.* **2** (3), 1378–1385.

Hu, M., Tian, H. & He, J. 2019 Unprecedented selectivity and rapid uptake of CuS nanostructures toward Hg(II) ions. *ACS Appl. Mater. Interfaces* **11**, 19200–19206.

Huang, L., He, M., Chen, B. & Hu, B. 2015 A designable magnetic MOF composite and facile coordination-based post-synthetic strategy for the enhanced removal of Hg^{2+} from water. *J. Mater. Chem. A* **3** (21), 11587–11595.

Jimenez-Falcao, S., Villalonga, A., Parra-Nieto, J., Llopis-Lorente, A. & Villalonga, R. 2020 Dithioacetal-mechanized mesoporous nanosensor for Hg(II) determination. *Micropor. Mesop. Mat.* **297**, 110054–110061.

Liew, R. K., Nam, W. L. & Chong, M. Y. 2018 Oil palm waste: an abundant and promising feedstock for microwave pyrolysis conversion into good quality biochar with potential multi-applications. *Process Saf. Environ.* **115**, 57–69.

Lin, G., Hu, T., Wang, S., Xie, T., Zhang, L., Cheng, S., Fu, L. & Xiong, C. 2019 Selective removal behavior and mechanism of trace Hg(II) using modified corn husk leaves. *Chemosphere* **225**, 65–72.

Lou, Z., Zhao, Z., Li, Y., Shan, W., Xiong, Y., Fang, D., Yue, S. & Zang, S. 2013 Contribution of tertiary amino groups to Re(VII) biosorption on modified corn stalk: competitiveness and regularity. *Bioresource Technol.* **133**, 546–554.

Luo, T., Tian, X., Yang, C., Luo, W., Nie, Y. & Wang, Y. 2017 Polyethylenimine-functionalized corn bract, an agricultural waste material, for efficient removal and recovery of Cr(VI) from aqueous solution. *J. Agric. Food Chem.* **65**, 7153–7158.

Mohammad, A., Hamed, E., Mahmood, K. A. & Alireza Abbaspourrad, A. 2018 Biocompatible nanodendrimer for efficient adsorption and reduction of Hg(II). *ACS Sustainable Chem. Eng.* **6** (10), 13332–13348.

Naushad, M., Ahamad, T., AlOthman, Z. A. & Al-Muhtaseb, A. H. 2019 Green and eco-friendly nanocomposite for the removal of toxic Hg(II) metal ion from aqueous environment: adsorption kinetics & isotherm modelling. *J. Mol. Liq.* **279**, 1–8.

Oveisi, F., Nikazar, M., Razzaghi, M. H., Mirrahimi, A. S. & Jafarzadeh, M. T. 2017 Effective removal of mercury from aqueous solution using thiol-functionalized magnetic nanoparticles. *Environ. Nano. Monitoring Manage.* **7**, 130–138.

Pala, I. R. & Brock, S. L. 2012 Zns nanoparticle gels for remediation of Pb^{2+} and Hg^{2+} polluted water. *ACS Appl. Mater. Interfaces* **4** (4), 2160–2167.

Qin, W., Qian, G., Tao, H., Wang, J., Sun, J., Cui, X., Zhang, Y. & Zhang, X. 2019 Adsorption of Hg(II) ions by PAMAM dendrimers modified attapulgite composites. *React. Funct. Polym.* **136**, 75–85.

Sadegh, H., Ali, G. M., Makhlouf, A. H., Chong, K. F., Alharbi, N. S., Agarwal, S. & Gupta, V. K. 2018 MWCNTs-Fe_3O_4

nanocomposite for Hg(II) high adsorption efficiency. *J. Mol. Liq.* **258**, 345–353.

Sun, Y., Lou, Z., Yu, J., Zhou, X., Lv, D., Zhou, J., Baig, S. A. & Xu, X. 2017 Immobilization of mercury (II) from aqueous solution using Al_2O_3-supported nanoscale FeS. *Chem. Eng. J.* **323**, 483–491.

Sun, J., Shen, Y. & Hu, X. 2018 Polyaniline/flower-like CuS composites with improved electromagnetic interference shielding effectiveness. *Polym. Bull.* **75**, 653–667.

Trikkaliotis, D. G., Christoforidis, A. K., Mitropoulos, A. C. & Kyzas, G. Z. 2020 Adsorption of copper ions onto chitosan/poly(vinyl alcohol) beads functionalized with poly(ethylene glycol). *Carbohyd. Polym.* **234**, 115890–115903.

Velempini, T. & Pillay, K. 2019 Sulphur functionalized materials for Hg(II) adsorption: a review. *J. Environ. Chem. Eng.* **7** (5), 103350–103371.

Wang, X., Lv, P., Zou, H., Li, Y., Li, X. & Liao, Y. 2016 Synthesis of poly(2-aminothiazole) for selective removal of Hg(II) in aqueous solutions. *Ind. Eng. Chem. Res.* **55** (17), 4911–4918.

Yang, M. & Zhou, R. 2012 Research on degumming experiment of corn bracts. *Adv. Mat. Res.* **550–553**, 1242–1247.

Yang, G., Han, H., Du, C., Luo, Z. & Wang, Y. 2010 Facile synthesis of melamine-based porous polymer networks and their application for removal of aqueous mercury ions. *Polymer* **51** (26), 6193–6202.

Yi, H., Zhang, X., Jia, F., Wei, Z., Zhao, Y. & Song, S. 2019 Competition of Hg^{2+} adsorption and surface oxidation on MoS_2 surface as affected by sulfur vacancy defects. *Appl. Surf. Sci.* **483**, 521–528.

Zhang, Z., Niu, Y., Chen, H., Yang, Z., Bai, L., Xue, Z. & Yang, H. 2019 Feasible one-pot sequential synthesis of aminopyridine functionalized magnetic Fe_3O_4 hybrids for robust capture of aqueous Hg(II) and Ag(I). *ACS Sustainable Chem. Eng.* **7**, 7324–7337.

Zhi, L., Zuo, W., Chen, F. & Wang, B. 2016 3D MoS_2 composition aerogels as chemosensors and adsorbents for colorimetric detection and high-capacity adsorption of Hg^{2+}. *ACS Sustainable Chem. Eng.* **4** (6), 3398–3408.

First received 5 January 2021; accepted in revised form 27 April 2021. Available online 10 May 2021